ATLAS High-Level Trigger Performance for Calorimeter-Based Algorithms in LHC Run-I

Alexander Mann, on behalf of the ATLAS collaboration

LMU LUDWIG-MAXIMILIANS-UNIVERSITÄT MÜNCHEN

The LHC Luminosity Challenge

Run-I of the Large Hadron Collider (LHC) comprises three data-taking periods within the years 2010 – 2012. Due to the very successful ramp-up of the instantaneous luminosity, the trigger algorithms had to be constantly adapted and improved in order to keep the rates within the given limits. In particular the calorimeter-based triggers had to cope with an increasing level of background activity from the increasing number of concurrent events (in-time pile-up). The great performance of the ATLAS trigger under these challenging conditions was a key element in the discovery of new physics such as the Higgs boson in 2012.

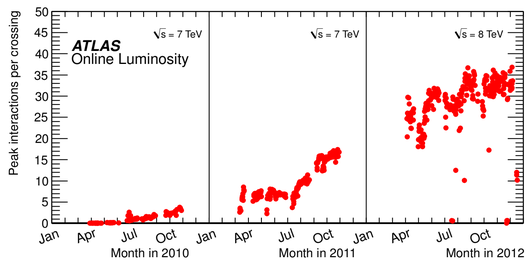

Peak level of in-time pile-up in pp-collisions during Run-I.

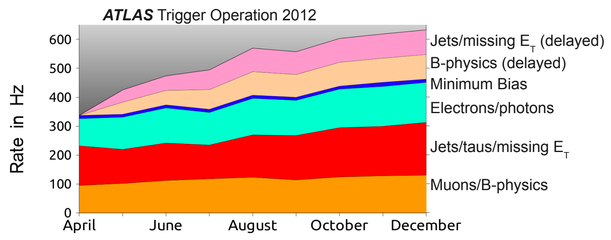

EF output rates in 2012, averaged over periods for which the LHC declared stable beams, for the regular data streams and the two delayed streams.

LHC conditions (proton-proton collisions)	Design	2010	2011	2012
Center-of-mass energy $\sqrt{s}$ (TeV)	14	7	7	8
Peak expected number of interactions per beam crossing	23 (avg.)	3	18	36
Peak instantaneous luminosity (Hz/cm^2)	10^{34}	$2 \cdot 10^{32}$	$3.9 \cdot 10^{33}$	$7.6 \cdot 10^{33}$
Peak number of proton bunches per beam	2808	348	1331	1380
Typical bunch spacing within a bunch train (ns)	25	150	50	50
Integrated luminosity recorded by ATLAS (1/fb)		0.045	5.08	21.3

The ATLAS Trigger and Data Acquisition System (TDAQ)

Design of the ATLAS trigger system

- three-level system
- seeded
  - definition of geometrical regions of interest (RoIs)
  - re-usage of results from previous steps
- step-wise manner
  - simple algorithms first, expensive ones last
  - early-rejection principle

Three-level structure

- Level 1 (L1)
  - hardware-based, runs on custom-built electronics
  - uses coarse-grained information from calorimeters and fast-response muon trigger chambers
  - no tracking possible, no topological cuts (during Run-I)
- Level 2 (L2)
  - software-based, runs on dedicated computing cluster
  - fetches full-granularity data from the RoIs defined at L1
  - adds tracking and topological cuts
  - L2 accept initiates event building (EB)
- Event Filter (EF)
  - software-based, runs on dedicated computing cluster
  - runs offline-like algorithms with access to complete event
- L2 + EF = High-Level Trigger (HLT)

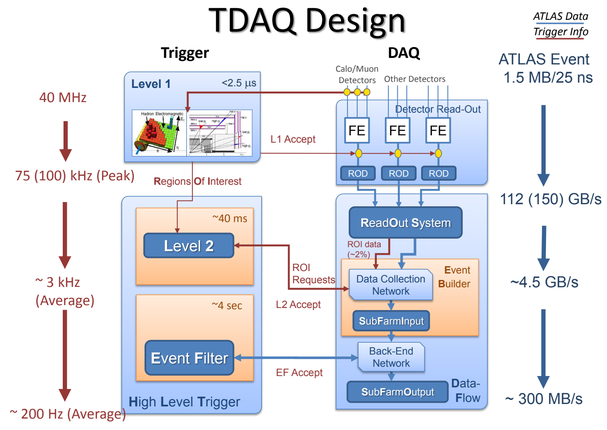

TDAQ working point	Design	2010	2011	2012
Peak L1 output rate (kHz)	75	20	50	70
Peak L2 output rate (kHz)	3.5	3.5	5.5	6.5
EF output rate (kHz)	0.2	0.35	0.4	0.7
L1 latency (µs)	< 2.5	< 2.5	< 2.5	< 2.5
L2 latency (ms)	40	40	45	75
EF processing time (s)	4	0.3	0.6	1
RoI data fraction (%)	2	5	5	10

Performance of the $E_{\mathrm{T}}^{\mathrm{miss}}$ Trigger

The $E_{\mathrm{T}}^{\mathrm{miss}}$ trigger is designed to select collision events with non-interacting particles. Being a global sum over the full calorimeter, this trigger is very susceptible to pile-up effects, leading to strong non-linearities in the low-threshold rates as function of luminosity, and posing a challenge for this type of trigger. Note that muon information is available at both L2 and EF, but was not included in the $E_{\mathrm{T}}^{\mathrm{miss}}$ computation in active 2011 triggers, and in 2012 only in one combined chain at EF level.

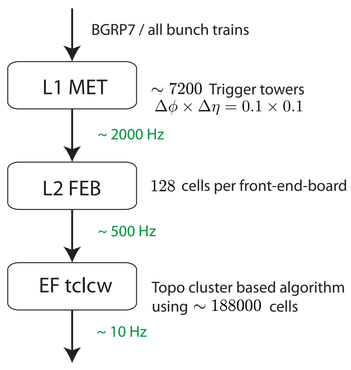

Structure of the $E_{\mathrm{T}}^{\mathrm{miss}}$ trigger in 2012

L2 improvements during Run-I

- in 2012: L2 uses **FEB-based** $E_{\mathrm{T}}^{\mathrm{miss}}$
  - before: L2 $E_{\mathrm{T}}^{\mathrm{miss}}$ = L1 $E_{\mathrm{T}}^{\mathrm{miss}}$
  - an upgrade of the ROS made it possible to collect cell-based summary information provided by the calorimeter front-end boards (FEB)

EF improvements during Run-I

- **noise suppression** and **pile-up correction** were introduced in May 2011
- 2012: a new algorithm, summing **calibrated topological clusters ("tclcw")**, replaced the cell-based algorithm with a one-sided noise cut

$E_{\mathrm{T}}^{\mathrm{miss}}$ significance trigger

- a new type of trigger (**XS trigger**) was implemented beginning of 2011
- makes use of the different scaling of real $E_{\mathrm{T}}^{\mathrm{miss}}$ (linear) and fake $E_{\mathrm{T}}^{\mathrm{miss}}$ (sqrt) with the scalar $\sum E_{\mathrm{T}}$
- used e. g. in combination with electron trigger to select W events
- rates are stable with increasing pile-up (rates of high XS thresholds may even slightly decrease for high pile-up)

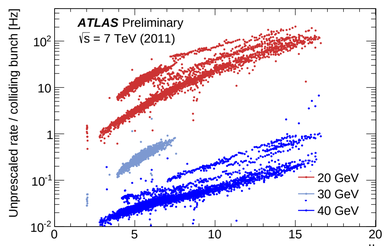

Rates per bunch crossing for low-threshold $E_{\mathrm{T}}^{\mathrm{miss}}$ triggers in 2011 as function of the number of concurrent interactions μ, illustrating the strong dependence on in-time pile-up.

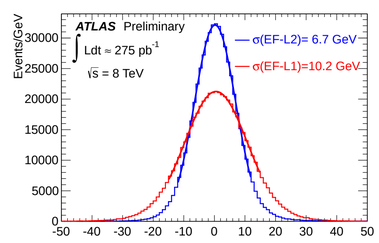

Resolution of E_x^{miss}, demonstrating the improvement of the **FEB-based** $E_{\mathrm{T}}^{\mathrm{miss}}$ at L2 in 2012 with respect to the L1 $E_{\mathrm{T}}^{\mathrm{miss}}$ value (based on a sum over trigger-towers) used before.

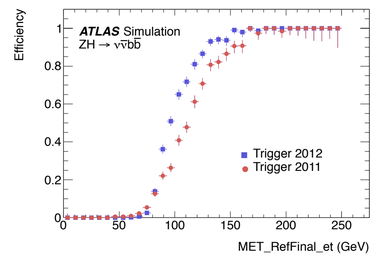

Efficiency of the lowest unprescaled chains in 2011 (thresholds: 50, 55, 60 GeV at L1, L2, EF) and 2012 (40, 45, 80 GeV with **tclcw**) as function of offline $E_{\mathrm{T}}^{\mathrm{miss}}$. Despite the harsher pile-up conditions in 2012, the trigger requirements are looser than in 2011, and the acceptance is considerably improved.

Performance of the Tau Trigger

The tau trigger selects hadronic decays of tau leptons, which are identified as collimated energy deposits in the calorimeters accompanied by one or a low number of matching charged tracks. In the HLT taus are selected based on cuts on track and cluster shape variables, optimized separately for one- or multi-prong taus.

L2 improvements during Run-I

- the **cone size** used in the computation of the L2 EM radius (the energy-weighted radius of the L2 tau candidate in the EM calorimeter) was changed from 0.4 (2011) to 0.2 (2012) to reduce pile-up dependence
- an additional **cut** $|\Delta z_0| < 2\,\mathrm{mm}$ was introduced in 2012 in the computation of $\sum p_{\mathrm{T}}$ of tracks to distinguish pile-up tracks from those coming from a tau decay

EF improvements during Run-I

- in 2011 the cut-based selection was optimized:
  - the selection of tracks was tightened
  - more shape variables were used, and the cuts were made dependent on E_{T} of the tau candidate as in the offline selection
  - the tau energy was computed from topological clusters with a local calibration scale instead of a global calibration scale as in 2010
- for 2012 the cut-based algorithm used before was replaced by a multi-variate algorithm using **boosted decision trees (BDT)** and pile-up robust input variables

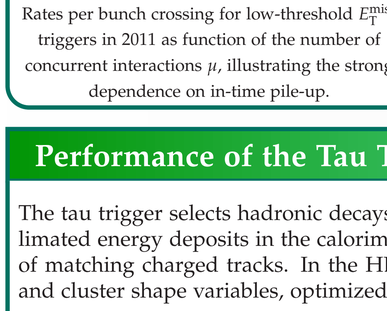

Marginal cut efficiency for tau candidates, showing the much lower pile-up dependence of the smaller **L2 cone size** used in 2012.

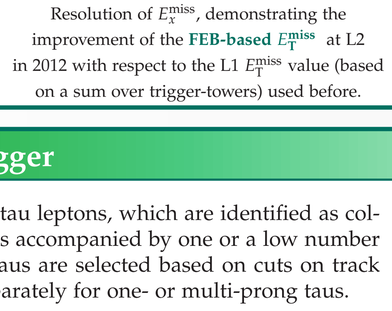

Pile-up dependence of the ratio of $\sum p_{\mathrm{T}}$ of tracks in the isolation region and tracks in the core region, showing that the $|\Delta z_0| < 2\,\mathrm{mm}$ requirement at L2 helps against pile-up effects.

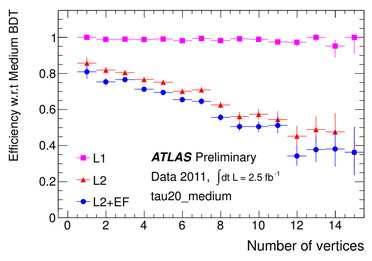

Efficiency in 2011: A severe performance degradation with increasing pile-up is observed.

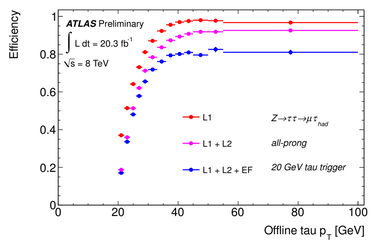

Efficiency in 2012, using a **BDT** algorithm at EF. The plots show that the measures to reduce the pile-up dependence observed in 2011 are effective.

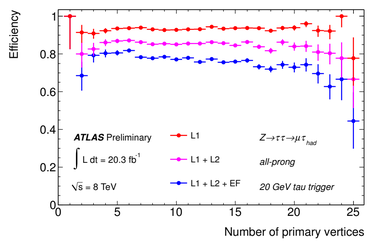

Ideas and Prospects for Run-II (2015 – 2018)

Anticipated LHC data-taking conditions

- center-of-mass energy increases to 13 TeV
- peak instantaneous luminosity reaches and possibly exceeds design value of $10^{34}\,\mathrm{Hz/cm^2}$
- more in-time pile-up: ~ 50 or more concurrent interactions
- more out-of-time pile-up: reduced bunch spacing of 25 ns
- an integrated luminosity of 75 – 100 fb^{-1} is delivered to ATLAS and CMS during three years of data-taking

Trigger strategy needs to be revisited

- both the higher instantaneous luminosity and the higher center-of-mass energy lead to higher trigger rates
  - trigger rates may scale faster than linear with pile-up
- algorithms need to become even more pile-up robust to avoid inefficiencies
  - isolation requirements need to be refined
  - triggers can move to tighter selections
  - multi-variate algorithms may be more widely used

Foreseen ATLAS TDAQ upgrades

- higher output bandwidth:
  L1 output up to 100 kHz, HLT up to 500 Hz, maybe more
- higher data access limit thanks to network upgrade and new ROS
- capability to define topological triggers already at L1
- L2, EB and EF will be merged, yielding unified HLT architecture with higher flexibility (which allows to do e. g. incremental event building, prefetching, caching)
- the hardware-based FastTracker system will be deployed:
  - provides track information at beginning of L2
  - may allow for primary vertex reconstruction

Further ideas

- L4 trigger: use Tier-0 reconstruction as a final trigger level
- Deferred Triggers: store subset of the events in the DAQ system, to be processed later during (between) fills
- Data Scouting: write out events with only trigger objects

Performance of the Jet Trigger

Jet triggers scan for collimated energy deposits in the calorimeters arising from the hadronization of high-energy quarks or gluons. These jets are the most common final-state object produced at the LHC with a large production cross-section. The original, entirely RoI-based design of the jet trigger has been upgraded and refined in several steps both at L2 and EF.

L2 improvements during Run-I

- **noise suppression** and **pile-up correction** were introduced in May 2011 (both at L2 and EF)
- for 2012 data-taking, the **L1.5 triggers** (also denoted as L2 full scan, **L2FS**), were activated:
  - instead of being seeded by L1 RoIs, all trigger towers are used as input with a (minimum) 0.1×0.1 granularity in $\eta \times \phi$
  - jet building is done with FastJet using an anti-k_t algorithm
  - solves the problem of efficiency loss of the RoI-based approach for events with many and close-by jets
  - L1.5 jets can be used directly in the L2 trigger decision or for seeding L2 RoI-based jet finding with higher resolution (L2PS)
- during 2012, a **L2 partial scan** (**L2PS**) was tested
  - works at cell level within previously defined RoIs (found by L1 or L2FS), uses anti-k_t to build jets
- finally, also a **hadronic calibration** of L2FS jets was tested

EF improvements during Run-I

- from the beginning of 2011, the **EF full scan (EFFS)** was used
  - provides unseeded jet finding using an anti-k_t algorithm
  - input: topological clusters formed from calorimeter cells
  - original RoI-based EF design thus was never used because EF jet algorithms were running in pass-through mode in 2010

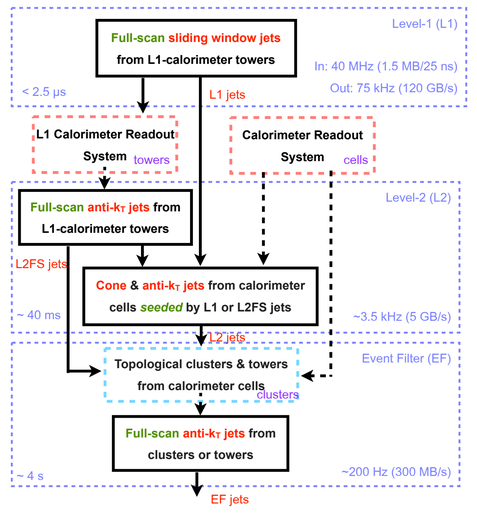

Structure of the ATLAS jet trigger in 2012

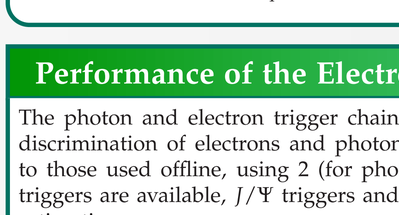

Position resolution for L1, L1.5, and L2 jet triggers. **L1.5** is comparable to L2 and significantly improves on L1.

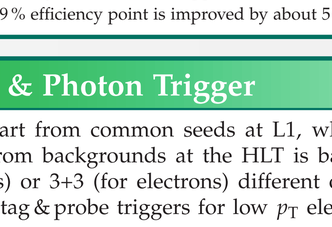

Efficiency of different 6-jet triggers in events with at least 6 offline jets with $E_{\mathrm{T}} > 30\,\mathrm{GeV}$. **L1.5** recovers efficiency lacking at L1 in multijet events.

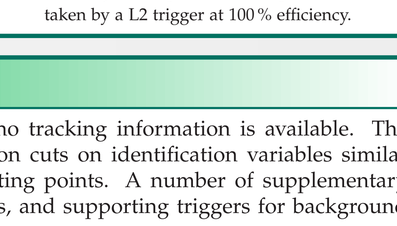

Efficiency of **L2FS** and **L2PS** 6-jet triggers in events with at least six offline jets jets with $E_{\mathrm{T}} > 30\,\mathrm{GeV}$. L2PS allows for a more efficient rejection by exploiting the full calorimeter granularity at cell level.

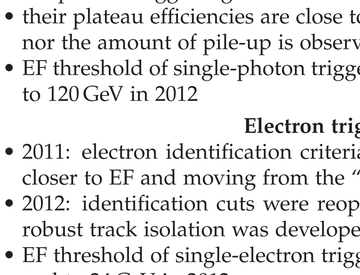

Efficiency of the primary HLT jet trigger in the 2011 heavy ion run ($\sqrt{s_{NN}} = 2.76\,\mathrm{TeV}$). Neither efficiency nor position resolution *(not shown)* are strongly dependent on the centrality of the Pb-Pb collisions thanks to an iterative baseline subtraction technique.

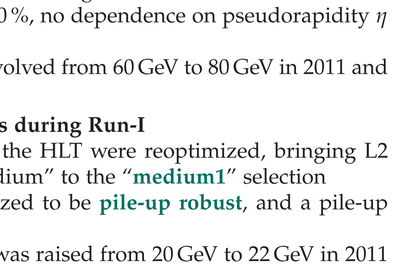

Efficiency for a single jet trigger chain with and without **noise suppression**. The effect is much larger at L2 because topological clustering at EF already includes noise suppression. The overall 99 % efficiency point is improved by about 5 GeV.

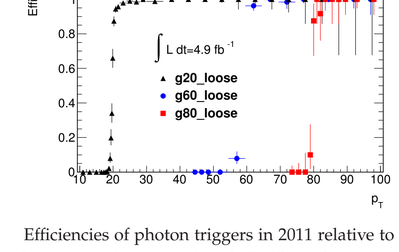

Efficiency for various Event Filter trigger chains calculated using the bootstrap method. For data, the efficiency is computed with respect to events taken by a L2 trigger at 100 % efficiency.

Performance of the Electron & Photon Trigger

The photon and electron trigger chains start from common seeds at L1, where no tracking information is available. The discrimination of electrons and photons from backgrounds at the HLT is based on cuts on identification variables similar to those used offline, using 2 (for photons) or 3+3 (for electrons) different operating points. A number of supplementary triggers are available, J/Ψ triggers and W-tag & probe triggers for low p_{T} electrons, and supporting triggers for background estimations.

Photon triggers during Run-I

- the photon trigger algorithms were stable throughout Run-I
- their plateau efficiencies are close to 100 %, no dependence on pseudorapidity η nor the amount of pile-up is observed
- EF threshold of single-photon trigger evolved from 60 GeV to 80 GeV in 2011 and to 120 GeV in 2012

Electron triggers during Run-I

- 2011: electron identification criteria at the HLT were reoptimized, bringing L2 closer to EF and moving from the "medium" to the "**medium1**" selection
- 2012: identification cuts were reoptimized to be **pile-up robust**, and a pile-up robust track isolation was developed
- EF threshold of single-electron trigger was raised from 20 GeV to 22 GeV in 2011 and to 24 GeV in 2012

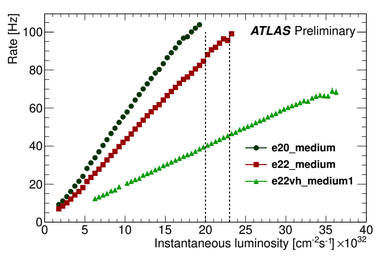

EF trigger rates for single-electron triggers in 2011, showing the achieved **reduction of rates**. "vh" refers to the modified L1 seed.

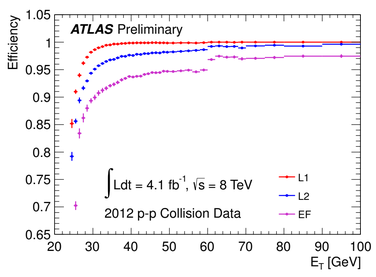

Efficiencies of single-electron triggers: e24vhi_medium1 OR e60_medium1.

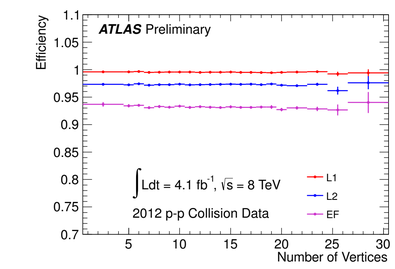

Efficiencies of single-electron triggers for offline electrons with $E_{\mathrm{T}} > 25\,\mathrm{GeV}$, demonstrating **robustness** against pile-up at all levels.

Efficiencies of photon triggers in 2011 relative to L1 seeds as function of "tight" offline photon p_{T}, exhibiting very sharp turn-on curves.